Multivoltaic GaSe<SmCl$_3$> clathrate as new hybrid functional nanostructure

Fedir IVASHCHYSHYN[1,2]*, Anna PIDLUZHNA[1], Dariusz CALUS[1], Orest HRYHORCHAK[3], Piotr CHABECKI[1], and Oleksandr MAKARCHUK[1,2]

[1] Czestochowa University of Technology, Al. Armii Krajowej 17, 42-200 Czestochowa, Poland,
[2] Lviv Polytechnic National University, Bandera 12, Lviv, 79013, Ukraine
[3] Ivan Franko Lviv National University, Cyril and Methodius 8, Lviv, 79005, Ukraine

Abstract. The electrical properties and behaviour in constant magnetic field of fourfold expanded *GaSe* matrix intercalated with SmCl$_3$ guest were investigated by means of impedance spectroscopy and cyclic voltammetry. It was determined that the synthesized *GaSe<SmCl$_3$>* clathrate of 4-fold expansion demonstrates the coexistence of mechanisms of generation, transformation and accumulation of electric energy on a quantum level. These mechanisms are driven from external sources of magnetic, thermal and electric field without Faradaic reactions. Therefore, investigated *GaSe<SmCl$_3$>* structure is of great attraction in multivoltaics as a prototype of new class of materials. Quantum mechanical model of electro motive force of spin nature is proposed. The main focus of work lies in the prospects of synthesized clathrates for the development of power nanosources and gyrator-free delay nanolines controlled by means of magnetic field.

Key words: impedance analysis; *GaSe*; multiferroic; thermogalvanic effect; negative capacity.

1. Introduction

Today's rapid development in nanoelectronics and spintronics upgrades to the problem of material functional hybridity, which takes a prominent position in the field of the novel circuitry solutions. In the foregoing perspective multiferroic materials are most widely studied. Multiferroic materials are substances where the ferroelectric and magnetic ordering coexists, which opens the prospects for the creation of new functional materials and nanodevices based on them [1–7].

On the other hand, nanodevices with autonomous operation mode require nanoscale power sources which are capable to convert the energy from a variety of external fields. Obviously, there is no other alternative to solve this problem than the transition to a new quantum level of energy storage, since the electrochemical method is unacceptable *a priori* in this case. Unfortunately, such tasks have only recently begun to be formulated. So, experts from Illinois University (USA) offered a system of vacuum nanotube arrays and called it Digital quantum battery. However, today this system exists in the form of theoretical calculations only [8]. Ilyanok A. suggested to use a thin dielectric layer at a large contact area, which can be realized in nanocomposites with the permittivity $\varepsilon = 2 \cdot 10^6$ [9]. Hai et al. [10] discovered the electromotive force of spin origin in a nanostructure with alternating magnetic and non-magnetic nanoparticles within which a tunnelling, that contained a large number of

quantum nanomagnets of a given composition, was formed. In this case, the magnetic energy was converted into electric during the process of magnetic quantum tunnelling. A spin capacitor based on field-effect transistor was suggested as well [11]. The electromotive force (EMF) of ~ 0.1 V in this capacitor was formed by spin-polarized injection. However, nowadays there are still no well-developed nanosources of energy. There is the idea and experimental attempts to confirm it [12], but with parameters and conditions that are far from commercial use. This work is devoted to finding the ways to overcome the problem.

2. Technological aspects and investigation methods

Gallium Selenide (*GaSe*) monocrystals of distinct layered structure, grown by Bridgman-Stockbarger method, were used as a host matrix material. It demonstrates p-type conductivity with optical band gap value of ~ 2 eV [13]. *GaSe* is a well-known material for its ability to accommodate guest particles in positions perpendicular to crystallographic *C* axis [14] within the range of Van der Waals interaction. The process of guest component insertion into specific intracrystalline places is called intercalation [15].

Samarium (III) Chloride (*SmCl$_3$*) was chosen as guest component because of its magnetic properties. All our previous attempts to insert *SmCl$_3$* directly into *GaSe* failed. Therefore, the three-stage intercalation and deintercalation technique described in detail in [16,17] was used to obtain a fourfold expansion of initial *GaSe* matrix first and *GaSe<SmCl$_3$>* clathrate

*e-mail: FedirIvashchyshyn@gmail.com

F. Ivashchyshyn, A. Pidluzhna, D Calus, O. Hryhorchak, P. Chabecki, and O. Makarchuk

then. The insertion process was controlled by precision gravimetric method.

X-ray investigations were carried out with DRON-3 diffractometer and in Cu–K_α ($\lambda = 1.5419$ Å) radiation monochromatized by the reflection from (111) plane of Ge monocrystal in X-ray beam propagation mode. The application of perfect Ge monocrystal and collimation system for initial and scattered beam enabled to start measurements from wave vector $s = 0.01$ Å^{-1} for collecting spectra of the small-angle scattering. 1 mm slit was placed in front of the detector, that corresponds to spatial separation of $\Delta(2\theta) = 0.03°$. The registration of scattered radiation was carried out in the scan mode in the angular range of $0.25 - 4.00°$ with a step of $0.05°$; exposure time – 100 s.

Impedance analysis was performed using AUTOLAB (Eco-Chemie, The Netherlands) measuring facility integrated with FRA-2 and GPES software. Measurements were executed within 10^{-3}–10^6 Hz frequency range perpendicularly to guest component planes. Questionable data points were removed employing Dirichlet filtering [18, 19]. Frequency dependences of complex impedance Z were analysed by a graph-analytic method in the ZView 2.3 (Scribner Associates) software package. Approximation errors did not exceed 4%. Impedance spectra were recorded under normal conditions (room temperature, darkness), as well as in a constant magnetic field that was applied perpendicularly to the sheets with magnetic field strength value of 2.75 kOe.

Thermostimulated depolarization spectra were recorded in the mode of short-circuited contacts with linear heating at a rate of 5°C/min.

3. Results and discussion

The values of corresponding interplanar distances d for synthesised clathrate were calculated on the basis of the analysis of the angular positions of the X-ray diffraction peaks, shifted to the small-angle region compared to the expanded matrix (Fig. 1). These calculations in combination with the small-angle X-ray scattering data confirm that the synthesized clathrate is one of the architectures with staged ordering (inset in Fig. 1). It should be noted that $GaSe<SmCl_3>$ clathrate is characterized by defective structure, which in particular manifests itself in some scattering in values of interlayer distance, the presence of microstresses and structural defects.

Figure 2 shows the frequency dependences of the real part of specific complex impedance (ReZ) measured perpendicularly to the layers of the expanded $GaSe$ matrix and synthesised $GaSe<SmCl_3>$ clathrate. The part of the real component of specific complex impedance that corresponds to the current flow caused by delocalised charge carriers differs drastically in the low frequency range and drops in one order of magnitude after $SmCl_3$ encapsulation. A positive magnetoresistance is visualized with a magnetic field application but in the $0.1 - 400$ Hz frequency range only.

The shape of Nyquist plot (the mapping of the complex impedance Z in the plane with real ReZ and imaginary – ImZ
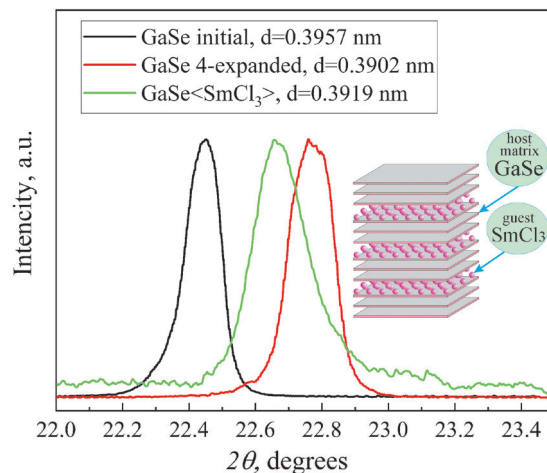

Fig. 1. XRD diffraction pattern of $GaSe$ initial sample (black), $GaSe$ fourfold expanded sample (red), $GaSe<SmCl_3>$ (green) clathrate with interlayer distances d. The inset represents a schematic structure of the clathrate architecture
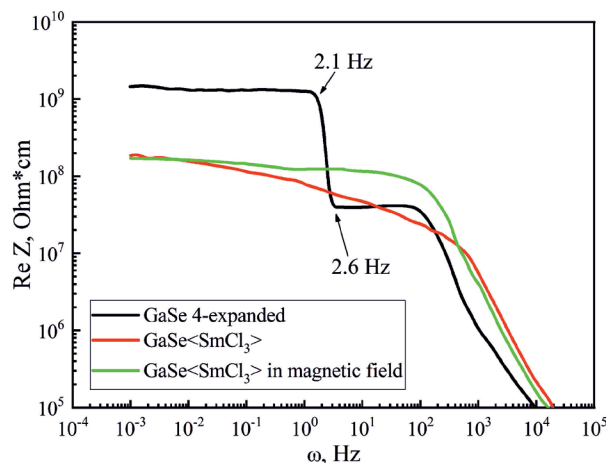

Fig. 2. Frequency dependences of real component of complex impedance, that is perpendicular to $GaSe<SmCl_3>$ nanosheets and which are measured under normal conditions (red) and in magnetic field (green). Black – initial expanded matrix

parts as the coordinate axes) changed significantly (Fig. 3). The horizontal branch of complex impedance is observed for initial expanded $GaSe$ matrix only (Fig. 3a) and disappears for $GaSe<SmCl_3>$ clathrate structure (Fig. 3b). This branch shows a sharp almost 40-fold decrease in the ReZ in a very narrow $2.1 - 2.6$ Hz frequency range (Fig. 2) and disappears for $GaSe<SmCl_3>$ most probably because of delocalisation of charge carriers from trap centres near the Fermi level stimulated by alternating field. But most extraordinary phenomena is observed when at low frequencies impedance goes in IVth quadrant of complex plane (Fig. 3). This effect is known as negative capacitance [20, 21] and is proposed to apply in nanoelectronics for developing gyrator free delay lines. The observed, in this work, inductive capacitance under magnetic field is more intense and has an inverse frequency genesis that enables magnetic operation by delay nanolines.
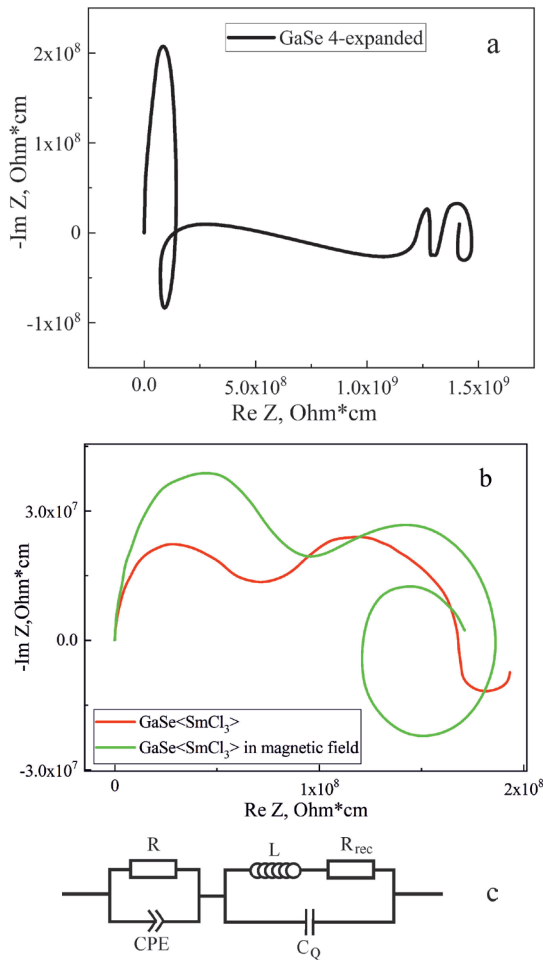
Fig. 3. Nyquist plots for the direction that is perpendicular to nanosheets of expanded *GaSe* matrix (a, black) and *GaSe<SmCl₃>* (b) which are measured under normal conditions (red) and in magnetic field (green). The equivalent electric circuit (c) for all diagrams

The equivalent electric circuit for the representation of impedance response is shown in Fig. 3c. The high frequency $R\|CPE$ link with *CPE* as constant phase element of capacitive type stands for distributed capacitance that is caused by vacancies or impurity levels which serve for the conduction of clathrate at room temperature. The lowest frequency unit $C_Q\|R_{rec}L$ simulates current flow through the host-guest interface [22] and L represents the inductance, R_{rec} is the recombination resistance for charging the quantum capacitance C_Q [23], which is determined by $C_Q = e^2 dn/dE_{Fn}$ with n as an electron density and E_{Fn} as an energy position of hole Fermi quasilevel. The admittance for low frequency region is described by the equation

$$Y(\omega) = \frac{1}{R_{rec} + i\omega L} + i\omega C_Q \qquad (1)$$

and at really low frequencies can be rewritten as

$$Y(\omega) = \frac{1}{R_{rec}} - i\omega C, \qquad (2)$$

where $C = C_L - C_Q$; $C_L = L/R_{rec}^2$.

According to Eq. (2) the impedance of the last unit of the equivalent electric circuit for nanohybrid material at low frequencies $(\omega < 1/(R_{rec}C))$ is the parallel connection of recombination resistance R_{rec} and constant negative capacitance C.

The spectrum of the thermostimulated discharge current for *GaSe<SmCl₃>* recorded at a constant temperature scan rate revealed significant bands of homocharge relaxation, alternating with vague bands of heterocharge relaxation (Fig. 4). Therefore, on the basis of theory for spontaneous thermovoltaic energy generation [24–28], the important conclusion can be made. The synthesised *GaSe<SmCl₃>* structure demonstrates an over twofold increase in generated electromotive force of thermovoltaic effect at room temperature and fourfold increase at temperatures over 315 K if compared to known structures.
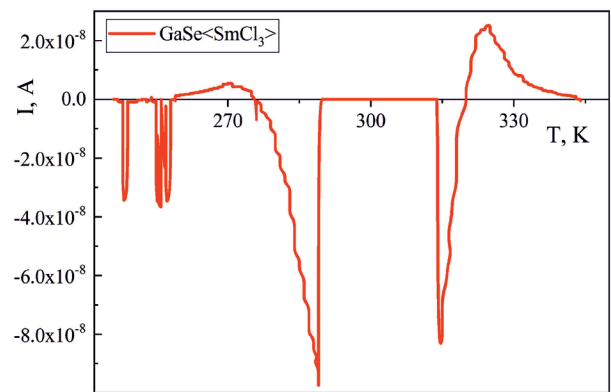

Fig. 4. Thermostimulated depolarization of the extended *GaSe<SmCl₃>*

The cyclic voltammogram of synthesised *GaSe<SmCl₃>* nanohybrid structure is untypical (Fig. 5) and illustrates the charge accumulation from extrinsic source and EMF of about 1.5 V appearances. The asymmetrical character for EMF in relation to applied voltage polarity can be provoked by thermogalvanic effect as well. Also, the change of current-voltage character in a magnetic field is an extraordinary phenomenon which is caused by spin EMF generation and confirmed by the values of voltage at zero current during (a–d, see Fig. 5) straight and forward scanning. The value of EMF caused by injected charges
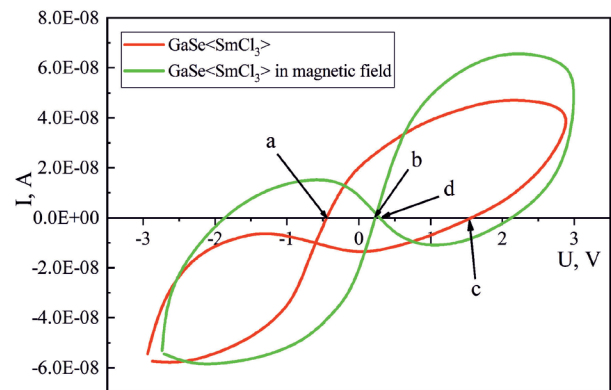

Fig. 5. Cyclic voltammetry characteristic of *GaSe<SmCl₃>* measured under normal conditions (red) and in magnetic field (green)

Bull. Pol. Acad. Sci. Tech. Sci. 69(2) 2021, e136726

3

in combination with thermovoltaic EMF changes of 0.75 V in an applied magnetic field and can be classified as spin EMF at room temperatures. This value is 30 times higher than EMF observed for nanostructure with magnetic tunnel junction at temperature of 3 K [10].

There is thorough understanding of physical mechanism for thermovoltaic phenomena (see [28]) but situation with spin EMF is more complicated and not so obvious because of not only inconsistency of Faraday's law of electromagnetic induction but because of basic conceptual approach. Let us look at the problem more thoroughly.

Consider the model of a spin capacitor which consists of two barriers of V_0 value and potential well between them. The material demonstrating these barriers is characterised by a large hysteresis which means that the direction of magnetization in the external magnetic field changes slowly, ideally indefinitely slowly. Instead, the electrons in the potential well can easily change the direction of their spin under the influence of the magnetic field. In the case of the absence of a magnetic field, spins of electrons within a potential well are oriented randomly, and when magnetic field is applied, they orient in its direction. It is an obvious fact that spins of electrons will suppress the influence of thermal motion, the intensity of which is characterized by the temperature value. However, taking into account the exclusively estimated nature of our calculations, we will ignore the influence of temperature.

Let us direct the axis z towards the magnetization of the material. Then eigenvectors of projection operator in direction l in the basis of the eigenvector of the operator σ_z: $|\uparrow>$ and $|\downarrow>$ are:

$$|\psi_l^+> = \cos(\theta/2)|\uparrow> + \sin(\theta/2)e^{i\varphi}|\downarrow>, \qquad (3)$$

$$|\psi_l^-> = -\sin(\theta/2)e^{-i\varphi}|\uparrow> + \cos(\theta/2)|\downarrow>, \qquad (4)$$

where θ and φ are the corresponding angles in the spherical coordinate system.

Then the probability that by measuring the projection of the spin on the l direction, we obtain a positive (negative) value, equal to:

$$p_l^\pm = |<\psi_l^\pm|\psi>|^2. \qquad (5)$$

In the case of magnetic field absence, the state vector ψ has the most general form, since there are no reasons for guiding the electron spin in a particular direction. Therefore, by averaging the values $p_l^\pm$ at angles θ and φ, we obtain that the probability of a positive (negative) value of the spin projection of an electron in an arbitrary direction, averaged over many dimensions, is equal to $1/2$

$$P^+ = P^- = \frac{1}{2}. \qquad (6)$$

This is a completely predictable result, since in the absence of a magnetic field there is no direction that would have been allocated.

If you apply a magnetic field, then all spin electrons in the well will be oriented in this direction. Let the direction of the magnetic field to form an angle χ with the direction of magnetization of the barriers. Then probabilities P^+ and P^- will be equal to

$$P^+ = \cos^2(\chi/2), \qquad P^- = \sin^2(\chi/2). \qquad (7)$$

and the energy of the particle in the well will be

$$E = E_1 \cos^2(\chi/2) + E_2 \sin^2(\chi/2), \qquad (8)$$

where E_1 is the energy of a particle in a potential well with walls of finite height V_0, and E_2 is the energy of a particle in a potential well with infinitely high walls, since with a negative projection magnitude on the direction of magnetization of barriers, the mentioned barriers become impenetrable to the particle. Let's find energy using the method of quantum impedance. In this case, the equation for finding its own energy levels has the form:

$$\tan(ka) = \frac{\cot(aeb)}{|Z_0/Z| - |Z/Z_0|} = \frac{\sqrt{E(V-E)}\cot(aeb)}{E - 0.5V}, \qquad (9)$$

where a is the width of potential well, and b is the width of barriers, Z and Z_0 are quantum mechanical impedances of potential barrier and potential well, respectively.

$$Z = 2\sqrt{2E/m}, \qquad Z_0 = 2\sqrt{2(E-V)/m}, \qquad (10)$$

$$k = i\frac{\sqrt{2mE}}{\hbar}, \qquad ae = \frac{\sqrt{2m(V-E)}}{\hbar}, \qquad (11)$$

For certainty we consider the ground state, considering that $V \gg E$

Then

$$\tan\left(\frac{\sqrt{2mE}}{\hbar}a\right) = 2\sqrt{\frac{E}{V}}\cot\left(\frac{\sqrt{2mV}}{\hbar}b\right). \qquad (12)$$

Let:

$$\frac{\sqrt{2mE}}{\hbar}a = x, \quad E = \frac{\hbar^2 x^2}{2ma^2} = \frac{x^2}{\alpha^2}. \qquad (13)$$

Then

$$\frac{\tan(x)}{x} = \frac{\cot\left(\alpha\sqrt{V}\frac{b}{a}\right)}{\alpha\sqrt{V}}. \qquad (14)$$

Numerically solving this equation for the given parameters a, b, and V_0 and finding the value x using which it is easy to calculate the average electron energy in the cell in the case of the absence of a magnetic field (E_0) and its presence (E_m)

$$E_0 = \frac{\hbar^2}{4ma^2}\left(x^2 + \pi^2\right), \qquad (15)$$

$$E_m = \frac{\hbar^2}{2ma^2}\left(x^2 \cos^2(\chi/2) + \pi^2 \sin^2(\chi/2)\right), \qquad (16)$$

4

Bull. Pol. Acad. Sci. Tech. Sci. 69(2) 2021, e136726

Accordingly, the difference in capacities is:

$$\Delta C = \frac{e^2}{2}\left(\frac{1}{E_0} - \frac{1}{E_m}\right) = \frac{ma^2e^2}{\hbar^2}\left(\frac{2}{(x^2+\pi^2)}\right.$$
$$\left. - \frac{1}{(x^2\cos^2(\chi/2) + \pi^2\sin^2(\chi/2))}\right). \qquad (17)$$

Thus, in the case of $\Delta C > 0$ there is the effect of energy accumulation in a magnetic field in the heterostructure, and in the case of $\Delta C < 0$ the EMF generation effect during a certain time appears and depends on the properties of the $GaSe<SmCl_3>$ clathrate.

4. Conclusions

The $GaSe<SmCl_3>$ clathrate synthesized by reintercalative technology with a four-fold expansion has the separated architecture of the third stage of ordering.

The intercalation of samarium trichloride is accompanied by the appearance of a low-frequency inductive response magnitude of which increases with a frequency-genesis inversion in a direct magnetic field of 2.75 kOe, that gives the possibility of creating non-giratory delay nanolines with magnetic control.

Synthesized $GaSe<SmCl_3>$ clathrate generates spontaneously EMF of up to ∼10 V, which by more than two orders of magnitude is larger at room temperature and about four times larger at temperatures above 315 K compared to other materials.

The coexistence of the thermovoltaic and spin EMF, the effect of the accumulation of charge from the external source in the $GaSe<SmCl_3>$ clathrate of the third stage of the separation, gives reasons for representing it as a prototype of a new class of substances as multivolaics, and with the functional hybridity of the inductive element.

The conditions under which the energy accumulation in a magnetic field or EMF generation effect during a certain time are discussed and assumed that they depend on the properties of the $GaSe<SmCl_3>$ clathrate.

References

[1] M.J. Fiebig, "Revival of the magnetoelectric effect", *Phys. D Appl. Phys.* 38, R123-R152 (2005).

[2] D.I. Khomskii, "Multiferroics: Different ways to combine magnetism and ferroelectricity", *J. Magn. Magn. Mater.* 306, 1–8 (2006).

[3] W. Eerenstein, N.D. Mathur, and J.F. Scott, "Multiferroic and magnetoelectric materials", *Nature*. 442, 759–765 (2006).

[4] Y. Tokura, "Materials science. Multiferroics as quantum electromagnets", *Science* 312(5779), 1481–1482 (2006).

[5] R. Ramesh and N.A. Spaldin, "Multiferroics: progress and prospects in thin films", *Nature Mater.* 6(1), 21–29 (2007).

[6] S. Cheong and M. Mostovoy, "Multiferroics: a magnetic twist for ferroelectricity", *Nature Mater.* 6(1) 13–20 (2007).

[7] A.P. Pyatakov and A.K Zvezdin, "Magnetoelectric and multiferroic media", *Phys.-Usp.* 55(6), 557–581 (2012).

[8] A.W. Hübler and O. Onyeama, "Digital quantum batteries: Energy and information storage in nanovacuum tube arrays", *Wiley Periodicals Inc. Complexity*. 15(5), 48–5 (2010).

[9] A. Ilyanok, "Quantum Supercapacitor", US Patent No. 7,193,261 B26, Mar. 20, 2007.

[10] N.H. Pham, O. Shinobu, T. Masaaki, E. Barnes Stewart, and M. Sadamichi, "Electromotive force and huge magnetoresistance in magnetic tunnel junctions", *Nature* 458, 489–493 (2009).

[11] S. Datta, "Proposal for a "spin capacitor"", *Appl. Phys. Lett.* 87(1), 013115(1–3) (2005).

[12] T. Popławski, I. Bordun, and A. Pidluzhna, "Thermo-, magneto- and photo- dependent electrical properties of hierarchical InSe<β-CD<FeSO₄>> supramolecular compound", *Bull. Pol. Acad. Sci. Tech. Sci.* 68(43), 361–366 (2020).

[13] Y. Wu, H.-R. Fuh, D. Zhang, C.Ó. Coileáin, H. Xu, J. Cho, and H.-C. Wu, "Simultaneous large continuous band gap tunability and photoluminescence enhancement in GaSe nanosheets via elastic strain engineering", *Nano Energy* 32, 157–164 (2017).

[14] R.M.A. Lies, "III–VI Compounds", in *Preparation and crystal growth material with layered structure*, pp 225–254, ed. R.M.A. Lies, D. Retdel, Publishing Company, Dordrecht-Boston, 1977.

[15] R.H. Friend and A.D. Yoffe, "Electronic properties of intercalation complexes of the transition metal dichalcogenides", *Adv. Phys*. 36(1), 1–94 (1987).

[16] I. Grygorchak, F. Ivashchyshyn, P. Stakhira, R.R. Reghu, V. Cherpak, and J.V. Grazulevicius, "Intercalated Nanostructure Consisting of Inorganic Receptor and Organic Ambipolar Semiconductor", *J. Nanoelectron. Optoelectron.* 8, 292–296 (2013).

[17] T.M. Bishchaniuk, *et al.*, "Electronic Processes and Energy Storage in Inorganic/Organic Nanohybrids", *Mol. Cryst. Liq. Cryst.* 589, 132–140 (2014).

[18] Z. Stoinov, B. Grafov, B. Savvova-Stoinova, and V. Yelkin, *Electrochemical Impedance*, Nauka, Moskow, 1991, [In Russian].

[19] *Impedance spectroscopy. Theory, experiment and application*, eds. E. Barsoukov and J.R. Macdonald, Wiley Interscience, Hoboken, New Jersey, 2005.

[20] J. Bisquert, H. Randriamahazaka, and G. Garcia-Belmonte, "Inductive behaviour by charge-transfer and relaxation in solid-state electrochemistry", *Electrochimica Acta* 51, 627–640 (2005).

[21] I. Mora-Seró, *et al.*, "Implications of the Negative Capacitance Observed at Forward Bias in Nanocomposite and Polycrystalline Solar Cells", *Nano Letters*. 6(4), 640–650 (2006).

[22] I.I. Grygorchak, F.O. Ivashchyshyn, M.V. Tokarchuk, N.T. Pokladok, and O.V. Viznovych, "Modification of properties of GaSe<β-cyclodexterin<FeSO₄>> clathrat by synthesis in superposed electric and light-wave fields", *J. Appl. Phys.* 121, 185501 (1–7) (2017).

[23] S. Luryi, "Quantum capacitance devices", *Appl. Phys. Lett.* 52, 501–503 (1988)

[24] V.V. Kaminskii and S.M. Solov'ev, "Emf induced by a change in the samarium ion valence as a result of a phase transition in SmS single crystals", *Phys. Solid State* 43, 439–442 (2001).

[25] V.V. Kaminskii and M.M. Kazanin, "Thermovoltaic effect in thin-film samarium-sulfide-based structures", *Tech. Phys. Lett.* 34, 361–362 (2008).

[26] I.A. Pronin, B.V. Donkova, D.T. Dimitrov, I.A. Averin, J.A. Pencheva, and V.A. Moshnikov, "Relationship between the photocatalytic and photoluminescence properties of zinc oxide doped with copper and manganese", *Semiconductors* 48, 842–847 (2014).

[27] L.K. Krasteva, *et al.*, "Synthesis and characterization of nanostructured zinc oxide layers for sensor applications", *Semiconductors* 47, 586–591 (2013).

[28] V.V. Kaminskii, L.N. Vasil'ev, M.V. Romanova, and S.M. Solov'ev, "The mechanism of the appearance of an electromotive force on heating of SmS single crystals", *Phys. Solid State* 43, 1030–1032 (2001).

Bull. Pol. Acad. Sci. Tech. Sci. 69(2) 2021, e136726

5